CANADIAN JOURNAL of EXPLORATION GEOPHYSICS
VOL. 39, NO. 1 (June 2014), P. 10-14

Dip-induced apparent anisotropy

Ye Zheng[1], John Bancroft[2], and Don Lawton[2]

[1] Geo-X Exploration Services Inc., 60, 805 – 5 Avenue SW, Calgary, Alberta, Canada T2P 0N6
[2] Department of Geoscience, University of Calgary, 2500 University Drive NW, Calgary, Alberta, Canada T2N 1N4

Abstract

Amplitude-based fracture analysis detects the amplitude variation with azimuth and assumes the variation is due to horizontal transverse isotropy induced by aligned vertical or subvertical fractures. However, a dipping reflector in an isotropic background medium can produce azimuthal amplitude variations as well, and the pattern of the variation is similar to that caused by anisotropy. In practice, the dip-induced deceptive amplitude variations with azimuth should be removed before fracture analysis.

Introduction

There are many fractured hydrocarbon reservoirs in the world. The fractures not only provide storage space to hold oil and gas in reservoirs, but also increase the permeability of reservoirs, or provide pathways for oil and gas flowing to well bores to be produced. On the other hand, cemented or mineralized fractures are barriers to oil and gas flow. Depiction of open fracture density and orientation is an important aspect of seismic reservoir characterization. It is important for geologists, geophysicists and reservoir engineers to have detailed maps of fracture density and orientation when they are making development plans for fractured reservoirs. Based on the fracture information, they can optimize their development plans accordingly and choose optimal locations for production and injection wells to maximize the economic value of the reservoirs.

Seismic PP reflection data can be used for fracture analysis. Crampin et al. (1980) extracted fracture information from P-wave velocity anisotropy. Thomsen (1988) discussed normal moveout (NMO) velocity in directions parallel and perpendicular to the strike direction of the fractures. Tsvankin (1997) derived the NMO velocity in an arbitrary direction. Lefeuvre (1994) first utilized amplitude variation with azimuth from PP reflection data to detect fractures. Rüger (1998) analyzed the theory of amplitude variation with azimuth for reflected waves, and many others (e.g. Lynn et al., 1996; Teng and Mavko, 1996; Gray and Head, 2000; MacBeth and Lynn, 2001; Zheng and Gray, 2002; Zheng et al., 2004, 2008) worked on seismic fracture analysis based on the azimuthal variation of reflection amplitude.

In isotropic media, when an incident angle is small (< 30°), the amplitude of the reflected seismic wave off an interface of two layers can be expressed as (Shuey, 1985):

$$R(\theta) = A + B\sin^2\theta \ . \qquad (1)$$

where θ is the average angle of the seismic wave incident on and emergent from the reflector. The AVO intercept is given by the coefficient $A = \frac{1}{2}\left(\frac{\Delta V_p}{V_p} + \frac{\Delta\rho}{\rho}\right)$ is the P-wave normal-incident reflectivity. The AVO gradient is given by

$$B = \frac{1}{2}\frac{\Delta V_p}{V_p} - 2\left(\frac{V_s}{V_p}\right)^2\frac{\Delta\rho}{\rho} - 4\left(\frac{V_s}{V_p}\right)^2\frac{\Delta V_s}{V_s}$$

V_p and V_s are the average P- and S-wave velocities of the upper and lower layers respectively and ρ is the average bulk density of the two layers. ΔV_p and ΔV_s are the differences in the P- and S-wave velocities of the two layers respectively, and $\Delta\rho$ is the difference in the bulk density between the two layers.

It is common to consider a fractured medium as an HTI (Horizontal Transverse Isotropic) medium. When the media are HTI, Rüger (1998, 2002) shows that the azimuthal variation of the reflection coefficients can be described by an expanded version of Shuey's equation. Then the AVO gradient, B, of equation (1) is composed of an azimuthally invariant term B^{iso} plus an anisotropic contribution B^{ani} multiplied by the squared cosine of the azimuthal angle between the seismic ray path and the normal direction of fracture strike,

$$R(\theta) = A + [B^{iso} + B^{ani}\cos^2\varphi]\sin^2\theta \ , \qquad (2)$$

where,

$$B^{iso} = \frac{1}{2}\frac{\Delta V_p}{V_p} - 2\left(\frac{V_s}{V_p}\right)^2\frac{\Delta\rho}{\rho} - 4\left(\frac{V_s}{V_p}\right)^2\frac{\Delta V_s}{V_s} \ ,$$

$$B^{ani} = \frac{1}{2}\left[\Delta\delta^{(v)} + 2\left(\frac{2V_s}{V_p}\right)^2\Delta\gamma\right] \ ,$$

where $\delta^{(v)}$ and γ are the Thomsen's anisotropic parameters for an HTI medium. $\Delta\delta^{(v)}$ is the difference in $\delta^{(v)}$, and $\Delta\gamma$ is the difference in γ between the upper and lower layers. φ is the angle between the shot-receiver direction and the direction of the axis of symmetry which is perpendicular to the fractures. $\delta^{(v)}$ is an indicator of P-wave anisotropy, which is the relative difference of the NMO velocity in the direction perpendicular to the fractures and the vertical velocity. The superscript v here is to indicate that it is for vertical fractures (HTI media). γ is the relative difference of the fast S-wave velocity (both wave propagation and particle motion in the directions parallel to the fractures) and the slow S-wave velocity (wave propagation in the direction perpendicular to the fractures).

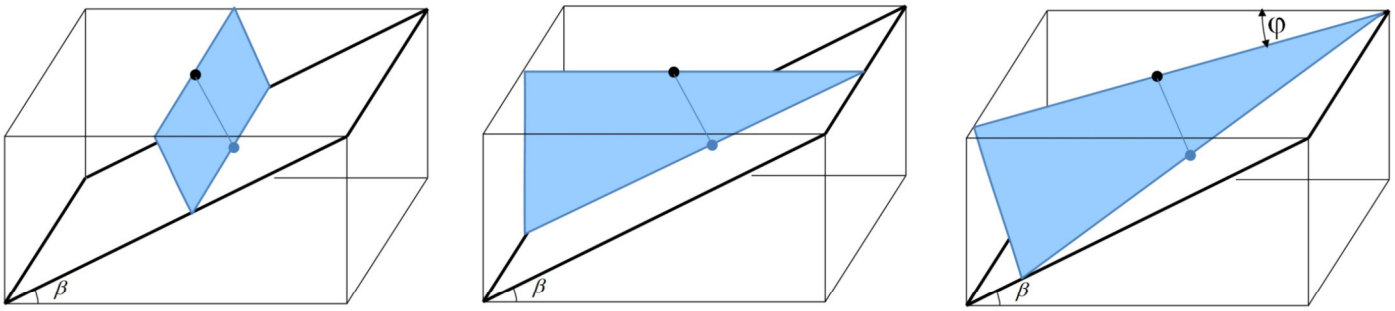

(a) (b) (c)

Figure 1. Three seismic lines with various azimuth, (a) strike line, (b) dip line, and (c) and arbitrary azimuthal line.

However, a dipping reflector in isotropic media can introduce azimuthal variation of the amplitude of seismic reflection waves which could be misinterpreted as "anisotropy". This deceptive amplitude variation with azimuth may mislead fracture analysis.

Consider an isotropic 3D volume with a dipping interface with three seismic lines with different azimuths passing through the same location on the surface, as illustrated in Figure 1. A surface location is identified by a black dot, with a corresponding zero-offset reflection point in the dipping plane identified by the blue dot. The line connecting these points is normal to the reflecting surface. The three seismic lines pass through the zero-offset location, are a strike line (a), a dip line (b), and an arbitrary azimuth line (c). The blue surface represents a plane that contains all the offset raypaths for the corresponding lines.

The offset traveltime T for the strike line in Figure 1(a) are computed with

$$T^2 = T_0^2 + \frac{4h^2}{V^2}, \qquad (3a)$$

where T_0 is the zero-offset traveltime, h the half source-receiver offset, and V the velocity of the medium. The plane of all the raypaths is normal to the dipping reflector.

The dip line in Figure 1(b) requires special attention to the velocities and the traveltime equation now becomes

$$T^2 = T_0^2 + \frac{4h^2\cos^2\beta}{V^2} = T_0^2 + \frac{4h^2}{V_{Stk-Dip}^2}, \qquad (3b)$$

where β is the dip angle of the interface and the stacking velocity, $V_{Stk\text{-}Dip}$ is defined with

$$V_{Stk-Dip} = V/\cos\beta .$$

All other lines with different azimuths φ, as illustrated in Figure 1c, will have stacking velocities that vary between V and $V^{Stk\text{-}Dip}$. Even though the velocity of the medium is constant and isotropic, the stacking velocities are dependent on the azimuth of a line, and may be mistakenly interpreted as anisotropy.

The purpose of the discussion associated with Figure 1 is to define the stacking velocity relative to the dip and source-receiver azimuth and relate it to the apparent amplitude anisotropy of a dipping event.

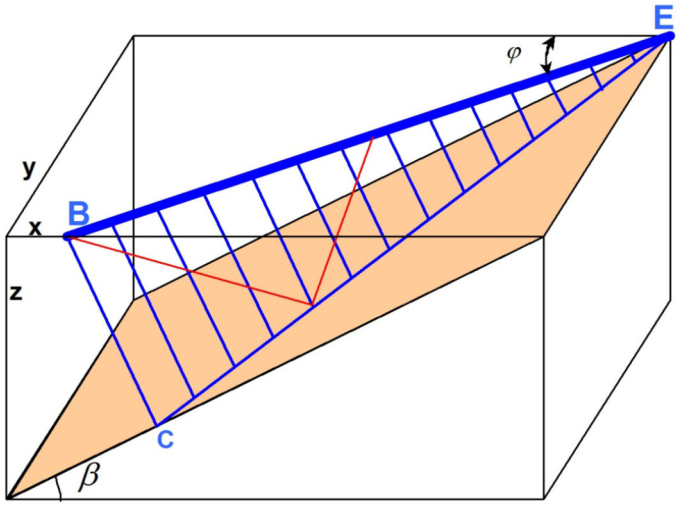

(a)

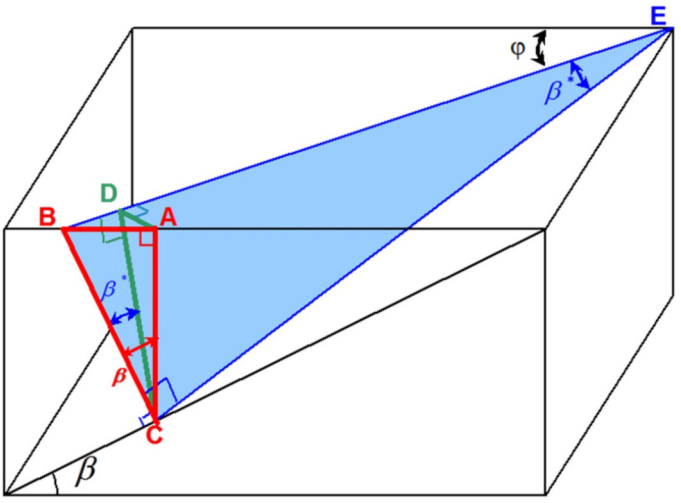

(b)

Figure 2. Geometry for defining the apparent dip for a 2D seismic line above a 3D dipping reflector, with (a) showing zero-offset normal incident raypaths, and (b) the geometry of a plane containing the offset raypaths.

Theory

A dipping reflector in isotropic media can introduce azimuthal variation of the amplitude of seismic reflection waves, in a similar pattern of that caused by azimuthally anisotropic media. For a given offset, the incident angle for the seismic wave traveling in the strike direction of the dip reflector is larger than that traveling in the dip direction. Therefore, for the same source-receiver offset, the amplitudes of the reflected seismic waves in the two directions are different, because the incident angles are different.

Levin (1971) derived an equation of the stacking velocity for a reflection from a dipping reflector. To extend his work, an equation of the amplitude variation versus offset and azimuth for a reflection from a dipping reflector is derived and presented here. Figure 2(a) shows a dipping reflector in a volume (x, y, z) with the dip β and the X-axis chosen to be parallel to the dip direction. The strike direction is parallel to the Y-axis. A 2D seismic line is defined on the surface by the blue line *BE* with an azimuthal angle φ referenced to the dip direction. All zero-offset raypaths will be normal to the dipping reflector with reflections points that lie on the line *CE*. All raypaths will lie on the plane defined by *BCE*.

As shown in Figure 2(b), *BC* is normal to the dipping reflector, *AC* normal to the acquisition surface (i.e., the z=0 plane) and the angle *ACB* is equal to β, and the angle *ABD* is φ. In the right-angle triangle *ABC*, by defining the distance *BC* as 1.0, then

$$AC = \cos\beta \ , \tag{4a}$$

$$AB = \sin\beta \ . \tag{4b}$$

The line *AC* is projected onto the plane *BCE* to produce the line *DC* that is normal to the 2D line on the surface *BE*. The length of *BD* is

$$BD = AB\cos\varphi = \sin\beta\cos\varphi \ . \tag{4c}$$

The triangles *BCD* and *BCE* are similar, therefore the angles *BEC* and *BCD* are the same, called β^*, which is the apparent dip angle of the dipping reflector with respect to the 2D seismic line *BE*, or

$$\sin\beta^* = \frac{BD}{BC} = \sin\beta\cos\varphi \ . \tag{4d}$$

Now the problem in 3D space is simplified to a problem in a 2D plane BCE (Figure 3) with an arbitrary azimuth φ. Assuming a source is at point *S*, and a receiver is at point *R*. The apparent dip angle of the reflector is β^*. *S′* is the mirror image of the source *S* with respect to the dip reflector. The angle between lines *SR* and *RN* is β^*. *M* is the midpoint between source *S* and receiver *R*, and MM_0 is normal to the reflector. Travel time for seismic waves from the source location, *S*, to the reflection point, *G*, and to the receiver location, *R*, is equivalent to travel time from *S′* to *R*. From the geometry shown in Figure 3, it is not difficult to find out the relationships between these line segments are

$$SN = x\sin\beta^* \ , \tag{5a}$$

$$SS_0 = d + \frac{1}{2}SN \ , \tag{5b}$$

$$SS' = 2SS_0 = 2d + x\sin\beta^* \ , \tag{5c}$$

$$RN = x\cos\beta^* , \tag{5d}$$

$$NS' = SS' - SN = 2d \ , \tag{5e}$$

$$RS' = \sqrt{NS'^2 + RN^2} = \sqrt{4d^2 + x^2\cos^2\beta^*} \ , \tag{5f}$$

where *d* is the distance from the midpoint *M* to the reflector(i.e., length of line MM_0); *x* is the source-receiver offset(i.e, length of *SR*). According to the cosine law, the incident angle, θ, can be written as

$$\cos\theta = \frac{SS'^2 + RS'^2 - x^2}{2\cdot SS'\cdot RS'} = \frac{2d}{\sqrt{4d^2 + x^2\cos^2\beta^*}} . \tag{6}$$

By substituting equation (4d) into (6), equation (6) becomes

$$\cos\theta = \frac{2d}{\sqrt{4d^2 + x^2 - x^2\sin^2\beta\cos^2\varphi}} . \tag{7}$$

Defining θ_0 as the incident angle for the flat reflector ($\beta = 0$) with the same offset, we can write

$$\cos\theta_0 = \frac{2d}{\sqrt{4d^2 + x^2}} \ , \tag{8a}$$

$$\sin\theta_0 = \frac{x}{\sqrt{4d^2 + x^2}} \ . \tag{8b}$$

After some manipulations, the incident angle for a dipping reflector can be written as

$$\sin^2\theta = 1 - \frac{\cos^2\theta_0}{1 - \sin^2\theta_0\sin^2\beta\cos^2\varphi} .$$

Therefore, for sufficiently small values of β and θ_0, one can write a first order approximation as,

$$\sin^2\theta = \sin^2\theta_0(1 - \cos^2\theta_0\sin^2\beta\cos^2\varphi). \tag{9}$$

where the relationship of $1/(1\text{-}x) \sim 1+x$ is used.

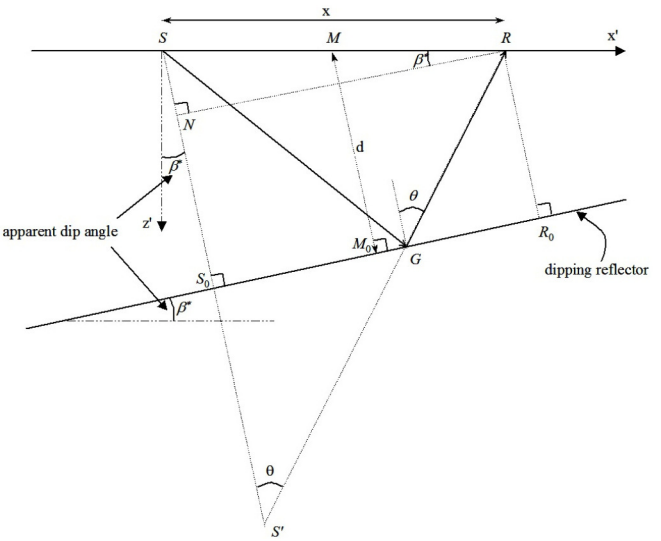

Figure 3. Geometry of a 2D seismic line with a dipping reflector.

Substituting equation (9) into Shuey's AVO equation (equation 1), the amplitude variation with incident angle and azimuth for the reflections from a dipping reflector is

$$R(\varphi) = A + B(1-\cos^2\theta_0 \sin^2\beta\cos^2\varphi)\sin^2\theta_0 . \quad (10)$$

By defining $B^* = -B\cos^2\theta_0\sin^2\beta$, equations (10) becomes in the same form as equation (2). In practice, when seismic data are being processed, there is no prior knowledge about whether the reflector is dipping or not. For a dipping reflector in an isotropic medium, the pattern of the amplitude variation with azimuth is similar to the pattern for a flat reflector in an anisotropic medium. Therefore, it is impossible to distinguish what causes the amplitude variation with azimuth. Thus, it is necessary to remove the dip effect before azimuthal AVO analysis. Common-angle prestack migration is a tool that can be used to remove the dip effect and preserve the true reflection angles which will be compromised by the industry standard common-offset migration (Zheng, 2006).

If the dip angle of reflectors is small, the amplitude variation with azimuth caused by the dipping reflectors might not be significant. However, when the dip angles are greater than 5°, the effect of the dipping reflectors cannot be ignored. Figure 4 shows an example of the amplitude variation with azimuth caused by a dipping reflector (30°) in an isotropic medium comparable to that caused by a flat reflector in an HTI anisotropic medium ($B^{ani} = 0.1$), which is equivalent to a moderately anisotropic medium with the $\delta^{(v)}$ of -0.05, and the γ of 0.08 for the velocities specified in the next paragraph).

Figure 4 showcases two earth models, one isotropic (Figure 4a) and the other HTI anisotropic (Figure 4b). Both models contain two layers and the upper layer is isotropic in both cases. The P-wave velocity is 3300 m/s in the upper layer and S-wave velocity 1500 m/s. The P-wave velocity is 3500 m/s in the lower layer and S-wave velocity 2333 m/s for the isotropic model. For the HTI anisotropic model, the lower layer P-wave velocity is 3500 and S-wave velocity 2333 m/s along the direction of fracture orientation. There is a dipping reflector with a dip angle of 30° in the isotropic model, while the HTI anisotropic model has a flat reflector and the anisotropic gradient, B^{ani}, is 0.1 (moderate anisotropy). Amplitude curves are calculated (using equation (10) for the isotropic model and equation (2) for the anisotropic model) at different incident angles (0°, 10°, 20° and 30°, respectively).

There are four pairs of curves in Figure 4(c). The red curves are the calculated reflection amplitudes from the flat reflector for the anisotropic medium; and the blue curves are the reflection amplitudes from the dipping reflector for the isotropic case. As shown in the figure, the red and blue curves match very closely. These two models create almost same amplitude response. If the dip effect is not removed before fracture analysis, it becomes difficult to distinguish whether the amplitude variation of azimuth is caused by azimuthal anisotropy or a dipping reflector.

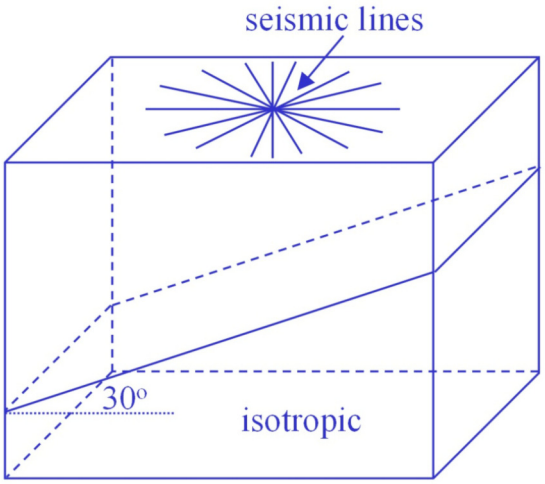

(a)

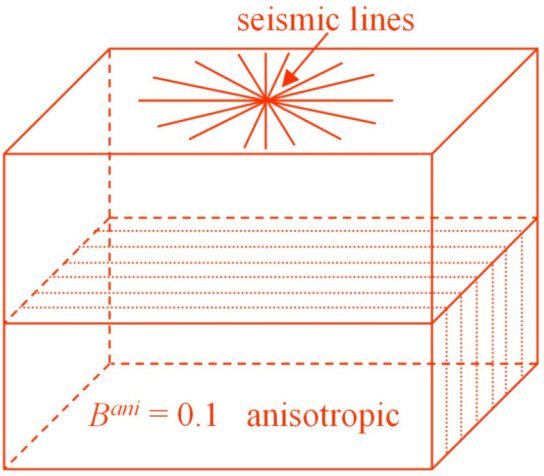

(b)

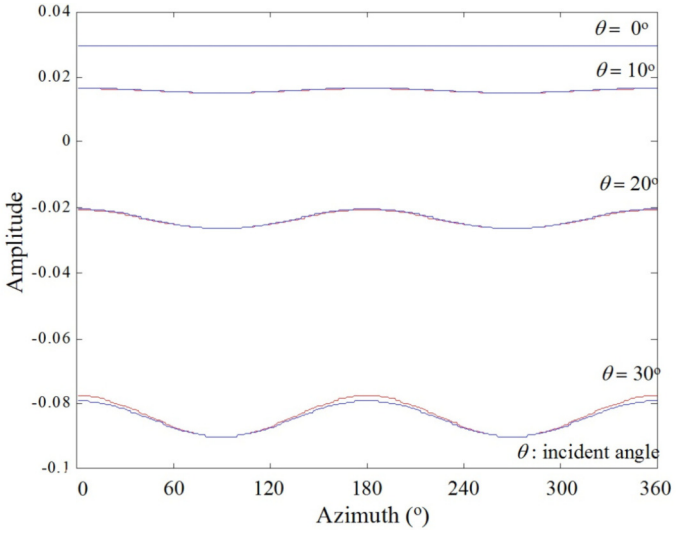

(c)

Figure 4. The comparison of amplitude from two models. One is (a) a dipping reflector in an isotropic medium, and another is (b) a flat reflector in an HTI medium. (c): Amplitude variations with azimuth from the two models are shown at four different incident angles (θ). Red curves show the amplitude from the HTI/flat reflector model, whereas the blue curves show the amplitude from the isotropic/dipping reflector model.

Conclusions

Theoretical analysis shows that the pattern of the reflection amplitude variation with azimuth caused by a dipping interface in isotropic media is very similar to the amplitude variation with azimuth caused by a flat interface in anisotropic media. The dip-induced deceptive "anisotropy" may mislead amplitude-based fracture detection in practice, since this type of fracture detection searches for azimuthal variation of amplitude and assumes the variation is caused by anisotropy. For stratigraphic areas, the deceptive "anisotropy" may not be a big problem. However, in structured areas, where dipping layers are expected, the apparent anisotropy must be eliminated, e.g. by common –angle prestack migration, before applying amplitude-based fracture detection.

References

Crampin, S., Evans, R., Üçer, B., Doyle, M., Davis, J.P., Yegorkina, G.V. and Miller, A., 1980, Observations of dilatancy-induced polarization anomalies and earthquake prediction: Nature, 286, 874 – 877.

Gray, F.D. and Head, K., 2000, Fracture detection in the Manderson Field: A 3-D AVAZ case history, 70th Annual International Meeting, SEG, Expanded Abstracts, 1413-1416.

Lefeuvre, F., 1994, Fracture related anisotropy detection and analysis: "And if the P□waves were enough?", 64th Annual International Meeting, SEG, Expanded Abstracts, 942-945.

Levin, F.K., 1971, Apparent velocity from dipping interface reflections: Geophysics, 36, 510-516.

Lynn, H.B., Simon, K.M., Bates, C. and Van Dok, R., 1996, Azimuthal anisotropy in P-wave (muiltiazimuth) data: The Leading Edge, 15, 923 – 928.

MacBeth, C. and Lynn, H., 2001, Mapping fractures and stress using full-offset full-azimuth 3D PP data, 71st Annual International Meeting, SEG, Expanded Abstracts, 110-113.

Rüger, A., 1998, Variation of P-wave reflectivity with offset and azimuth in anisotropic media: Geophysics, 63, 935 - 947.

Rüger, A., 2002, Reflection Coefficients and Azimuthal AVO Analysis in Anisotropic Media: Geophysical Monograph Series, Number 10, Soc. of Expl. Geophys.

Shuey, R.T., 1985, A simplification of Zoeppritz equations: geophysics, 50, 609 – 614.

Teng, L. and Mavko, G., 1996, Fracture signatures on P wave AVOZ: 66th Annual International Meeting, SEG, Expanded Abstracts, 1818 – 1821.

Thomsen, L.A., 1988, Reflection seismology over azimuthally anisotropic media: Geophysics, 53, 304 – 313.

Tsvankin, I., 1997, Reflection moveout and parameter estimation for horizontal transverse isotropy: Geophysics, 62, 614-629.

Zheng, Y., 2006, Seismic azimuthal anisotropy and fracture analysis from PP reflection data: Ph.D. Dissertation, The University of Calgary.

Zheng, Y. and Gray, F.D., 2002, Integrating seismic fracture analysis with migration: 72nd Annual International Meeting, SEG, Expanded Abstracts, 1642-1645.

Zheng, Y., Todorvic-Marinic, D. and Larson, G., 2004, Fracture detection: ambiguity and practical solution: 74th Annual International Meeting, SEG, Expanded Abstracts, 1575-1578.

Zheng, Y., Wang, J. and Perz, M., 2008, Pitfalls and tips for seismic fracture analysis: 78th Annual International Meeting, SEG, Expanded Abstracts, 27, no. 1, 1531-1535.